Journal of
Computational and Theoretical Nanoscience
Vol. 5, 528–534, 2008

RESEARCH ARTICLE

Reliability Analysis of Carbon Nanotubes Using Molecular Dynamics with the Aid of Grid Computing

Shaoping Xiao[1,*], Shaowen Wang[2], Jun Ni[3], Ransom Briggs[3], and Maciej Rysz[4]

[1] *Department of Mechanical and Industrial Engineering and Center for Computer-Aided Design (CCAD), The University of Iowa, Iowa City, IA 52242, USA*
[2] *Grid Research and EducatiOn Group @ ioWa (GROW), The University of Iowa, Iowa City, IA 52242, USA*
[3] *Grid Research and EducatiOn Group @ ioWa (GROW), Department of Computer Science, The University of Iowa, Iowa City, IA 52242, USA*
[4] *Department of Mechanical and Industrial Engineering, The University of Iowa, Iowa City, IA 52242, USA*

The first molecular dynamics simulation-based reliability analysis of carbon nanotubes is conducted in this paper. Instead of uncertainties of loads, we consider uncertainties of defects, especially vacancies, at the nanoscale in our modeling and simulation. A spatial Poisson point process is employed to assist randomly locating vacancies on the surface of nanotubes. With the aid of Grid computing technologies, a large number of molecular dynamic simulations are conducted to obtain statistical properties of nanotube strength and stress for reliability analysis. Reliabilities of nanotubes at various temperatures are also discussed.

Keywords: Nanotube, Defects, Reliability, Grid Computing.

1. INTRODUCTION

In the forefront research fields of nanotechnology, carbon nanotubes (CNTs) have been proposed as an ideal foundation of the next generation of materials and devices due to their unique mechanical and electrical properties. Studies have shown that CNTs have large interfacial area per volume and possess large tensile moduli and high thermal conductivity.[1–3] The Young's moduli and strengths of CNTs were predicted to be up to 1 TPa and 300 GPa, respectively. In addition, the thermal conductivity of a CNT could be 6600 W/m K. Therefore, they have been employed as ideal fibers for manufacturing novel nanocomposite materials with mechanical and thermal management applications.[4,5] In addition, nanotubes have become key components in nanodevice design.[6–8] Some devices have extraordinary characteristics, such as high oscillation frequency and low friction. With the development of nanotube technology, the reliability of CNTs is an inescapable issue to be thoroughly studied for further reliability analyses of novel nanotube-based composites and devices.

Although CNTs were predicted to have high strength,[9] the experiments conducted by Yu et al.[10] indicated such high strength could not be reached. The measured failure stresses were in the range of 10 GPa to 63 Gpa, while the measured failure strains varied from 2% to 14%. The measured failure stresses are far below what were predicted via theoretical analysis,[3] 300 GPa, and numerical simulations,[9] ~100 GPa. In addition, the large variance in the experimental measurements implies there were uncertainties not only on external loads but also on the testing samples. Those uncertainties include tube size, chirality, defects, and others. Researchers studied the effects of some uncertainties, including tube size, on the mechanical properties of CNTs. Natsuki et al.[11] studied both single-walled nanotubes (SWNTs) and multi-walled nanotubes (MWNTs) with a structural mechanics approach. They found that the Young's modulus of an SWNT decreased with the increasing tube diameter. In addition, Xiao and Hou[12] pointed out that such size effects were insignificant for CNTs with large diameters.

Some researchers considered the effects of defects on the mechanics of CNTs and their applications in nanocomposites and nanodevices. Defects, including chemical, topological, and vacancy defects, on CNTs can arise from various causes. Chemical defects consist of atoms/groups covalently attached to the carbon lattice of the tubes, as in oxidized carbon sites or chemical vapor deposition. Chemical defects usually occur during functionalizing CNTs in order to form chemical bonds between CNTs and the matrix in nanocomposites. Consequently, the mechanical properties of nanocomposites can be significantly enhanced because of the strong interfacial load transfer.[13] However, we don't think that functionalization

*Author to whom correspondence should be addressed.

1546-1955/2008/5/528/007 doi:10.1166/jctn.2008.012

will have significant effects on the mechanical properties of the nanotube itself. Topological defects correspond to the presence of rings other than hexagons and were mainly studied as pentagon/heptagon pairs.[14] However, topological defects also resulted in high failure strength[14] in comparison with the experimental measurements.[10]

Vacancy defects may have been caused through impact by high energy electrons in the TEM environment,[15] or may be defects in the original outer nanotube shell. Vacancy defects are modeled by taking out some atoms, called missing atoms, and then reconstructing carbon–carbon bonds. Consequently, such defects will form nanoscale cracks or holes, which can have large variations in size. Therefore, vacancy defects have significant impact on the mechanics of CNTs. In research performed by Milke et al.,[16] the role of vacancy defects and holes in the fracture of CNTs was studied. Both quantum mechanical and molecular mechanics calculations indicated that the holes due to one- and two-atom vacancy defects could reduce failure stresses by as much as ~26%. Xiao and Hou[17] studied the fracture of defected CNTs and their embedded nanocomposites. They concluded that vacancy defects in nanotubes could also dramatically reduce the failure stresses and strains of nanotube-embedded composites. In addition, they found that small volume of vacancy-defected CNTs might not reinforce but rather weaken their embedded composites. Furthermore, vacancy defects could influence mechanisms of nanotube-based devices. Xiao et al.[6] illustrated that a larger fraction of vacancy defects could induce larger interlayer friction in double-walled nanotube-based co-axial oscillators and that the oscillation of oscillators could cease more quickly. They also found that frequencies of nanotube-based resonant oscillators were reduced due to the existence of vacancies.[8]

Although the effects of defects on mechanics of nanotubes have been studied, most studies considered only that a vacancy defect existed in the middle of the nanotube. Uncertainties of vacancy defects on nanotubes, including the number and the location of defects, were not considered. In this paper, we consider two uncertainties related to vacancy defects: the number and the location of missing atoms, which determine the number and location of vacancy defects. We employ a homogeneous Poisson point process to determine the occurrence probability of a specified number of Poisson points, i.e., missing atoms. Furthermore, we assume that missing atoms occur on carbon nanotubes in a completely random manner. Consequently, nanotubes having the same number of missing atoms may have various numbers and locations of defects. Since those uncertainties are discrete, a large number of repeated simulations are required to study the reliability of a nanotube. A Grid computing environment is used in this paper to efficiently conduct simulations that are computationally intensive.

The outline of this paper is as follows. In Section 2, we discuss how to deal with uncertainties of vacancy defects on nanotubes. The computational model via molecular dynamics simulation for studying mechanics of nanotube is described in Section 3. Grid computing technologies employed in this paper is introduced in Section 4. We then study reliability of nanotubes based on simulation results in Section 5 and present conclusions in Section 6.

2. UNCERTAINTIES OF VACANCY DEFECTS ON NANOTUBES

We consider the following two uncertainties: the number and the location of missing atoms for vacancy defects. In this paper, we employ a homogeneous Poisson point process to determine the number of Poisson points (missing atoms). Due to the unique structures of single-walled carbon nanotubes, they can be mapped onto two-dimensional (2D) graphene planes with a thickness of 0.34 nm. Therefore, a 3D model can be simplified as a 2D surface problem. The probability of the number (k) of Poisson points occurring in a finite 2D plane is written as:

$$P(N(A) = k) = \frac{e^{-\lambda A}(\lambda A)^k}{k!}, \quad k = 1, 2, 3 \ldots \qquad (1)$$

where A is the plane area; $N(A)$ is the number of Poisson points on this area A; and λ is the Poisson point density per area. $N(A)$ and λ are also taken as the number of missing atoms and the missing atom density, respectively, in this paper. It is clear that different missing atom densities will result in different probability distributions of the number of missing atoms.

To randomize locations of vacancy defects, we first assume that the Poisson points are randomly distributed on a 2D plane to which the surface of a nanotube can be mapped. The atom that is the closest to a Poisson point is indicated as the missing atom. After the missing atoms are located, a defect site is denoted as the location containing one or several missing atoms neighboring each other. The number of missing atoms in a defect site results in the type of the generated vacancy defect after taking out the missing atoms and reconstructing bonds. The formed vacancy defects include one-atom vacancy defects, two-atom defects, and cluster-atom vacancy defects.[16, 18]

As an example, we conduct the generation of vacancy defects on a (10,0) nanotube with a missing atom density of 0.8 nm^{-2}. The surface area of the considered (10,0) nanotube is 12 nm^2. Figure 1 shows the probability distribution of the number of missing atoms determined via Eq. (1). We can see that the numbers of missing atoms are in the range of 0 to 20, and each number of missing atoms has its own probability of occurrence. For instance, the occurrence probability of 13 missing atoms is about 7%. In other words, if 100 computational samples are chosen to study the statistical properties of mechanical behavior of vacancy-defected nanotubes with $\lambda = 0.8$ nm^{-2}, there must be seven samples containing 13 missing atoms.

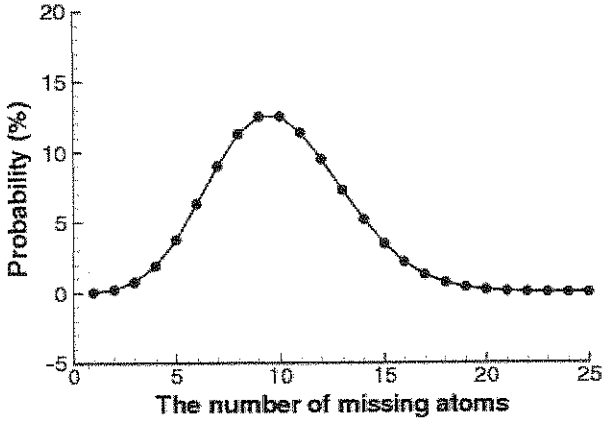

Fig. 1. Probability distribution of the number of missing atoms.

In one sample containing 13 missing atoms, 13 Poisson points are deposed onto a 2D plane to which the surface of the considered (10,0) nanotube is mapped. The coordinates of each Poisson point are randomly selected within this 2D plane, as shown in Figure 2(a). Next, we mark the closest carbon atom to each Poisson point as a missing atom, as illustrated in Figure 2(a). If more than one atom has the identical least distance to one Poisson point, the missing atom is randomly selected. Finally, we perform bond reconstruction[16, 18] to generate corresponding vacancy defects. Figure 2(b) shows that resulted vacancy defects include three one-atom vacancy defects (marked as "1a," which is symmetric, and "1b," which is asymmetric), three two-atom vacancy defects (marked as "2"), and one cluster-atom vacancy defect (marked as "3").

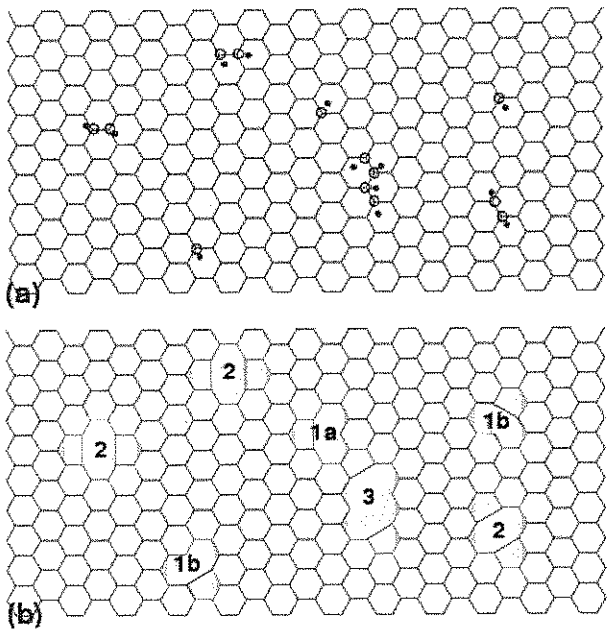

Fig. 2. Generation of vacancy defects on the surface of a (10,0) nanotube. (a) Deposition of Poisson points (dots) and selection of missing atoms (circles); (b) formation of vacancy defects.

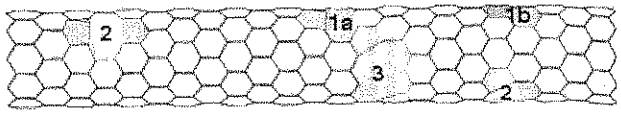

Fig. 3. The vacancy-defected (10,0) nanotube corresponding to Figure 2.

The configuration of the corresponding (10,0) zigzag nanotube is shown in Figure 3.

3. COMPUTATIONAL MODEL

For any given defected nanotube, molecular dynamics simulation is performed to investigate its stress–strain relation and strength. In molecular dynamics simulations, the following equations of motion are solved for the whole simulated system without the consideration of external forces:

$$m_I \ddot{\mathbf{d}}_I = -\mathbf{f}_I = -\frac{\partial E}{\partial \mathbf{x}_I} \tag{2}$$

where m_I is the mass of atom I, $\mathbf{x}_I$ is its position, and $\mathbf{x}_I = \mathbf{X}_I + \mathbf{d}_I$ ($\mathbf{X}_I$ is the original position of atom I and $\mathbf{d}_I$ is its displacement). $\mathbf{f}_I$ is the atomic force applied on atom I, and it is calculated from the first derivative of the potential, $E(\mathbf{x})$. Periodic boundary conditions are applied. A Hoover thermostat[19] is implemented so a constant temperature can be maintained during molecular dynamics simulations.

In this paper, we employ the modified Morse potential function[9] to describe interatomic interaction in CNTs. This potential can be written as:

$$\begin{aligned} E &= E_{\text{stretch}} + E_{\text{angle}} \\ E_{\text{stretch}} &= D_e\left\{\left[1 - e^{-\beta(r-r_0)}\right]^2 - 1\right\} \\ E_{\text{angle}} &= \frac{1}{2}k_\theta(\theta-\theta_0)^2\left[1 + k_s(\theta-\theta_0)^4\right] \end{aligned} \tag{3}$$

where E_{stretch} is the bond energy due to bond stretching or compressing, E_{angle} is the bond energy due to bond angle-bending, r is the current bond length, and θ is the angle of two adjacent bonds representing a standard deformation measure in molecular mechanics. The parameters are:

$$\begin{aligned} r_0 &= 1.42 \times 10^{-10}\ \text{m}, & D_e &= 6.03105 \times 10^{-19}\ \text{Nm} \\ \beta &= 2.625 \times 10^{10}\ \text{m}^{-1}, & \theta_0 &= 2.094\ \text{rad} \\ k_\theta &= 1.13 \times 10^{-18}\ \text{Nm/rad}^2, & k_s &= 0.754\ \text{rad}^{-4} \end{aligned} \tag{4}$$

It has been shown that this potential function results in reasonable Young's modulus and Poisson's ratio of nanotubes compared with experimental investigations.

In this paper, we mainly consider (40,0) zigzag nanotubes with the diameter of 16.4 nm and the length of 73.8 nm because (40,0) nanotubes are large enough to neglect size effects on mechanical properties of nanotubes

(see details given by Xiao and Hou[12]). Before the molecular dynamics simulation, the equilibrium state of nanotubes needs to be obtained via energy minimization. During the molecular dynamics simulation, the periodic boundary condition is employed with prescribed displacements. For each displacement increment, 0.7 nm, the tube was equilibrated for 1000 time steps. Another 100 time steps are used to calculate the time-averaged potential. The corresponding external force F can be calculated as the slope of the potential-displacement relation. Then, one can obtain the stress via $\sigma = F/(\pi D h)$, where D is the tube diameter and h is the tube thickness, i.e., 0.34 nm.

Algorithm 1 Nanotechnology application pseudo-code

```
dist ⟵ generatePoissonDistribution()
for i = 0 to numRuns do
  numMissingAtom[i] ⟵ dist.drawPoisson()
end for
5: for i = 0 to numRuns do
  nanotube ⟵ startWithNewNanotube()
  for j = 0 to numMissingAtom[i] do
    (x, y) ⟵ nanotube.randomPoint()
    nanotube.addDefect(x, y)
10: end for
  nanotube.testStrength()
end for
```

Fig. 4. Pseudo-code for calculating strengths of nanotubes.

4. GRID COMPUTING ENVIRONMENT AND PERFORMANCE

In this paper, we consider uncertainties of vacancy defects on carbon nanotubes and study reliability of nanotubes. For each nanotube sample, we conduct molecular dynamics simulation as described in the previous section to obtain stress–strain relations to identify mechanical properties of the simulated nanotube. The strength of a nanotube is determined as the stress when the nanotube fails subject to tension. Since uncertainties of vacancy defects are discrete, a large number of samples need to be simulated to obtain accurate statistical properties. In this paper, we plan to conduct 500 simulations on each case. Every simulation may run for a couple of hours to obtain the result, leading to a large overall computational runtime. We tackle this challenge of computational intensity using Grid computing technologies.

Grid computing technologies allow heterogeneous resources from multiple administrative domains to be dynamically aggregated, and thus to create a single supercomputing environment for computationally intensive applications.[20] Individual administrative domains may reside within the scope of a single physical site or a Virtual Organization (VO) for collaborative problem solving. Scalable Grids are often built on a number of VOs that allow dynamic membership of computational resources and users. For example, the Open Science Grid (OSG, http://www.opensciencegrid.org) is operated by the OSG Consortium, a partnership of over 50 universities and national laboratories that work together to create a global Grid-based cyberinfrastructure for scientific research and education. Currently, the OSG consists of more than two dozen VOs. We used the OSG for the computational experiments presented in this paper.

Our reliability analysis can be treated as a parameter sweep application from a Grid computing perspective by simultaneously evaluating different parameters using multiple resources. Specifically, the key to taking advantage of OSG computing power is to decompose the application at line 5 of the analysis pseudo-code, shown in Figure 4, into a number of relatively independent computing jobs and submit these jobs to multiple sites for parallel processing. Each job is executed with local data,

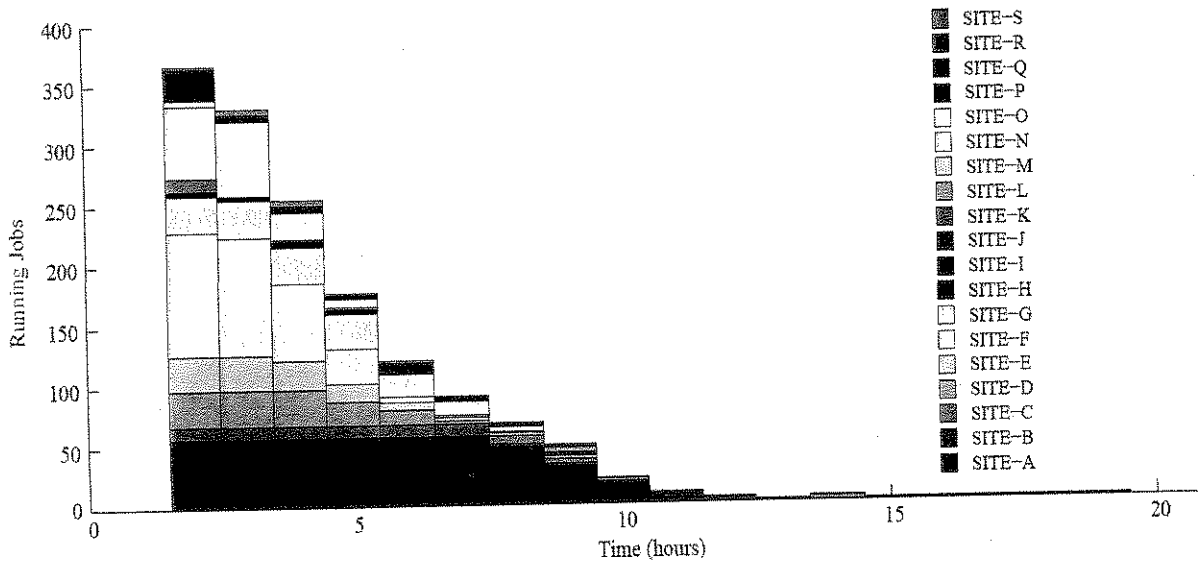

Fig. 5. Computation throughput using the Open Science Grid.

RESEARCH ARTICLE

which contains a subset of the Poisson points to simulate. Our computational experiments using OSG demonstrated that within 20 hours, we were able to finish a reliability analysis that could take over two months of computational runtime using a single desktop PC.

Specifically, Figure 5 shows the dynamics of executing computations at OSG sites as time progresses. In total, resources from 19 OSG sites were used. It took less than 20 hours to finish this run of computation for the analysis scenario presented in this paper. At the beginning stage of the computation, the number of active jobs decreased rapidly as most of selected sites completed individual jobs within the computation progress. After 10 hours, a small number of jobs remained unfinished, which can be explained by their low priority enforced by local resource management tools such as Condor (http://www.cs.wisc.edu/condor/). The overall computation throughput is significant and stable given dynamic changes of resource availability in our numerical simulations. In aggregate, our computational experiments have demonstrated that a significant high-throughput has been achieved for supporting the analyses to use OSG resources opportunistically.

5. RESULTS AND DISCUSSION

In this paper, we assume that the missing atom density, λ, follows the Gaussian distribution, i.e., the normal distribution, with the mean value $\mu_\lambda = 2.5$ nm^{-2} and the standard deviation $\hat{\sigma}_\lambda = 1.0$ nm^{-2}. The probability density function of the random variable λ follows:

$$f(\lambda) = \frac{1}{\hat{\sigma}_\lambda \sqrt{2\pi}} \exp\left[-\frac{1}{2}\left(\frac{\lambda - \mu_\lambda}{\hat{\sigma}_\lambda}\right)^2\right] \quad (5)$$

Equation (5) determines the probability of the missing atom density. Then, Eq. (1) is employed to determine the probability of the number of missing atoms.

We first investigate reliability of carbon nanotubes at the room temperature of 300 K. The histogram of nanotube strength based on 500 simulations is shown in Figure 6. It can be seen that the histogram matches the one from the experiments by Yu et al.[10] It should be noted that the experimental result was based on 19 measurements. Figure 6 also shows that the strength, S_Y, follows three-parameter Weibull distribution,[21] and its probability density function is written as:

$$f(S_Y) = \left(\frac{\beta_Y}{\eta_Y}\right)\left(\frac{S_Y - \gamma_Y}{\eta_Y}\right)^{\beta_Y - 1} \exp\left(-\frac{S_Y - \gamma_Y}{\eta_Y}\right)^{\beta_Y} \quad (6)$$

where β_Y is known as the shape parameter, η_Y is the scale parameter, and γ_Y is the location parameter. Based on the data we simulated, the parameters in Eq. (6) for the nanotube strength are: $\eta_Y = 15.0$ GPa, $\beta_Y = 2.0$, and $\gamma_Y = 11.0$ GPa. β_Y is 2.0 so that the Weibull distribution is specialized to the Rayleigh distribution.

The reliability of a nanotube is the probability that the nanotube will not fail in use. In other words, it is the probability that the applied load does not exceed the nanotube strength. Mathematically,[22] the reliability of a nanotube can be calculated as

$$R = \Pr(S_Y > s) = 1 - \Pr(S_Y \leq s) \quad (7)$$

where s is the applied load, which is the stress in this paper. Consequently, the following equation is derived:

$$R = 1 - e^{-((s-\gamma)/\eta)^\beta} \quad (8)$$

For instance, the reliability of a nanotube at the stress of 30 Gpa is calculated as 20.2%, as shown in the shaded area in Figure 7. In other words, the probability of failure for nanotubes subject to 30 Gpa is 79.8%.

It has been shown that temperature has significant effects on the strength of carbon nanotubes.[17] Consequently, there is the effect of temperature on the reliability of nanotubes. Similar to the experiment described above, we simulate 500 samples at 1000 K and 3000 K, respectively, to obtain the statistical properties of nanotube strength. The probability distributions of nanotube strength

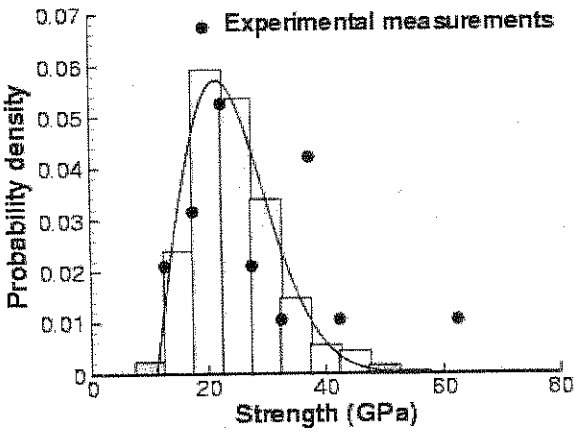

Fig. 6. Probability distribution of nanotube strength at the room temperature of 300 K.

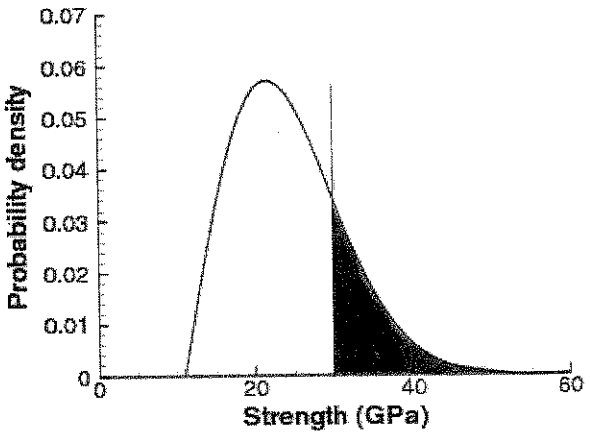

Fig. 7. Reliability of nanotubes at 30 Gpa at the room temperature of 300 K.

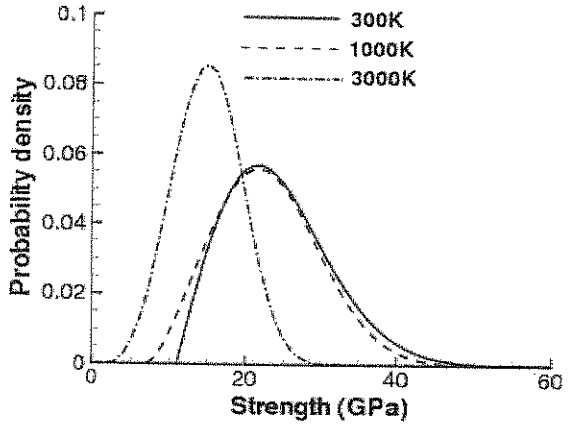

Fig. 8. Probability distribution of nanotube strength at various temperatures.

at various temperatures are shown in Figure 8. All of them follow the Weibull distribution. It can be seen that the reliability of a nanotube subject to a specific load is lower at a higher temperature. For instance, the reliabilities of nanotubes subject to a load of 30 Gpa stress are 20.2%, 16.8%, and 0.03% at 300 K, 1000 K, and 3000 K, respectively.

When nanotubes are subject to a specific elongation, the calculated stresses may be various due to randomly located vacancy defects. In this paper, we consider (40,0) nanotubes subject to 3% strain. The calculated stress, σ_s, also follows the Weibull distribution with the following three parameters: $\eta_S = 14.4$ GPa, $\beta_S = 3.9$, and $\gamma_S = 7.0$ GPa at the temperature of 300 K. Figure 9 illustrates the probability density distributions for the strength and stress, respectively. The reliability is calculated as follows:

$$R = \Pr(S_Y > \sigma_S) = 1 - \Pr(S_Y \le \sigma_S)$$
$$= 1 - \int_0^\infty \exp\left\{-u - \left[\frac{\eta_Y}{\eta_S} u^{1/\beta_Y} + \left(\frac{\gamma_S - \gamma_Y}{\eta_S}\right)\right]^{\beta_S}\right\} du \quad (9)$$

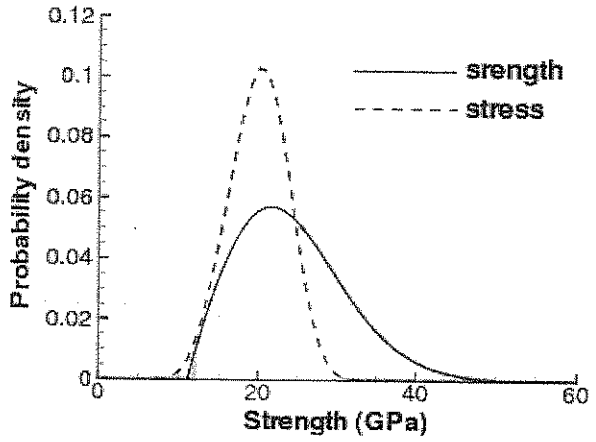

Fig. 9. Probability distributions of strength and stress corresponding to 3% strain at the room temperature of 300 K.

where $u = ((\sigma_Y - \gamma_Y)/\eta_Y)^{\beta_Y}$. Using the numerical integration methods, the above integral can be computed. Consequently, the reliability of nanotubes subject to 3% strain is 33.6%. In Figure 9, the shaded interference region indicates the probability of failure, which is 66.4%. At the temperatures of 1000 K and 3000 K, the reliabilities of nanotubes subject to 3% strain are 30.2% and 10.1%, respectively. We can have the same conclusion that the reliability of carbon nanotubes is lower at a higher temperature.

6. CONCLUSIONS

In this paper, we reported the first study on the reliability of carbon nanotubes. The considered uncertainties at the nanoscale include the number and location of vacancy defects. The Poisson point process was employed to describe those uncertainties. Once a sample, i.e., a carbon nanotube with randomly located vacancy defects, was generated, we performed molecular dynamics simulations to compute strength and/or stress. To accurately obtain statistical properties of output strength/stress, a large number of samples needed to be simulated. Consequently, molecular dynamics simulations were repeated and time consuming. The Open Science Grid was used here as an alternative solution since it enabled a large number of simulations to run simultaneously through the Internet. Based on our simulation results, the output nanotube strength followed the Weibull distribution and had a good agreement with experimental outcomes. Consequently, the reliability of nanotubes subject to a particular load could be computed as the probability that the nanotube strength was larger than the load. When nanotubes were subjected to a specific strain, the calculated stress was also a random variable due to the uncertainties of vacancy defects. Then, the reliability of nanotubes could be calculated from the interference region. We studied the temperature effect and found that a higher temperature resulted in a lower reliability of nanotubes.

Acknowledgments: This research was done using resources provided by the Open Science Grid, which is supported by the National Science Foundation and the U.S. Department of Energy's Office of Science. Xiao also acknowledges support from the Army Research Office (Contract: # W911NF-06-C-0140).

References

1. Q. Z. Zhao, M. B. Nardelli, and J. Bernholc, *Phys. Rev. B* 65, 144105 (**2002**).
2. J. P. Small, L. Shi, and P. Kim, *Solid State Commun.* 127, 181 (**2003**).
3. B. I. Yakobson, C. J. Brabec, and J. Bernholc, *Phys. Rev. Lett.* 76, 2511 (**1996**).
4. C. Wei, D. Srivastava, and K. Cho, *Nano Lett.* 2, 647 (**2002**).
5. R. H. Baughman, A. A. Zakhidov, and W. A. de Heer, *Science* 297, 787 (**2002**).

6. S. P. Xiao, D. Andersen, R. Han, and W. Hou, *J. Comput. Theor. Nanosci.* 3, 142 (**2006**).
7. D. Srivastava, *Nanotech.* 8, 186 (**1997**).
8. S. P. Xiao and W. Y. Hou, *Phys. Rev. B* 75, 125414 (**2007**).
9. T. Belytschko, S. P. Xiao, G. C. Schatz, and R. Ruoff, *Phys. Rev. B* 65, 235430 (**2002**).
10. M. F. Yu, O. Lourie, M. J. Dyer, K. Moloni, T. F. Kelly, and R. S. Ruoff, *Science* 287, 637 (**2000**).
11. T. Natsuki, K. Tantrakarn, and M. Endo, *Appl. Phys. A* 79, 117 (**2004**).
12. S. P. Xiao and W. Y. Hou, *Fullerenes Nanotubes Carbon Nanostruct.* 14, 9 (**2006**).
13. H. Geng, R. Rosen, B. Zheng, H. Shimoda, L. Fleming, J. Liu, and O. Zhou, *Adv. Mater.* 14, 1387 (**2002**).
14. B. I. Yakobson, *Appl. Phys. Lett.* 72, 918 (**1998**).
15. F. Banhart, *Rep. Prog. Phys.* 62, 1181 (**1999**).
16. S. L. Mielke, D. Troya, S. Zhang, J. Li, S. P. Xiao, R. Car, R. S. Ruoff, G. C. Schatz, and T. Belytschko, *Chem. Phys. Lett.* 390, 413 (**2004**).
17. S. Xiao and W. Y. Hou, *Phys. Rev. B* 73, 115406 (**2006**).
18. W. Y. Hou and S. P. Xiao, *J. Nanosci. Nanotechnol.* 7, 4478 (**2007**).
19. W. G. Hoover, *Phys. Rev. A* 31, 1695 (**1985**).
20. I. Foster, C. Kesselman, and S. Tuecke, *Int. J. High Perform. Comput. Appl.* 15, 200 (**2001**).
21. D. Kececioglu, Reliability and Life Testing Handbook, Prentice Hall, Inc., New Jersey (**1993**).
22. S. H. Dai and M. O. Wang, Reliability Analysis in Engineering Applications, Van Nostrand Reinhold, New York (**1992**).

Received: 10 April 2007. Accepted: 26 May 2007.

RESEARCH ARTICLE